JBC Papers in Press. Published on April 8, 2003 as Manuscript M302680200

Colocalization of ATP release sites and ecto-ATPase activity at the extracellular surface of human astrocytes

Sheldon M. Joseph, Marisa R. Buchakjian, and George R. Dubyak
School of Medicine
Department of Physiology and Biophysics
Case Western Reserve University
Cleveland, OH 44106 USA

Running Title: *Localized ATP Release from Astrocytes*

Key Words: Extracellular nucleotides, ATP release, astrocytes, P2 receptors, luciferase, ecto-ATPase, protease-activated receptor, hypotonic stress.

Send correspondence to: George R. Dubyak, School of Medicine, Department of Physiology and Biophysics, E565, Case Western Reserve University, Cleveland, OH 44106 USA

Email **gxd3@po.cwru.edu**

SUMMARY

Extracellular ATP and other nucleotides function as autocrine and paracrine signaling factors in many tissues. Recent studies suggest that P2 nucleotide receptors and ecto-nucleotidases compete for a limited pool of endogenously released nucleotides within cell surface microenvironments that are functionally segregated from the bulk extracellular compartment. To test this hypothesis, we have used luciferase-based methods to continuously record extracellular ATP levels in monolayers of human 1321N1 astrocytoma cells under resting conditions, during stimulation of Ca^{2+}-mobilizing receptors for thrombin or acetylcholine, and during mechanical stimulation by hypotonic stress. Soluble luciferase was utilized as an indicator of ATP levels within the bulk extracellular compartment, while a chimeric protein A-luciferase, adsorbed to antibodies against a GPI-anchored plasma membrane protein, was used as a spatially localized probe of ATP levels at the immediate extracellular surface. Significant accumulation of ATP in the bulk extracellular compartment, under either resting (1-2 nM ATP) or stimulated (10-80 nM ATP) conditions, was observed only when endogenous ecto-ATPase activity was pharmacologically inhibited by the poorly metabolizable analog, βγ-methylene ATP. In contrast, accumulation of submicromolar ATP in the cell surface microenvironment was readily measured even in the absence of ecto-ATPase inhibition suggesting that the spatially colocalized luciferase could effectively compete with endogenous ecto-ATPases for released ATP. Other experiments revealed a critical role for elevated cytosolic $[Ca^{2+}]$ in the ATP release mechanism triggered by thrombin or muscarinic receptors, but not in basal ATP release or release stimulated by hypotonic stress. These observations suggest that ATP release sites are colocalized with ecto-ATPases at the astrocyte cell surface. This co-localization may act to spatially restrict the actions of released ATP as a paracrine or autocrine mediator of cell-to-cell signaling.

INTRODUCTION

ATP and other nucleotides function as intercellular signaling molecules when released to extracellular compartments. Genes encoding seven ionotropic P2X nucleotide receptor subtypes (1), eight G protein-coupled P2Y nucleotide receptor subtypes (2, 5) and at least nine different ecto-nucleotidases (3, 4) have been identified in human and other vertebrate genomes. Most mammalian cell types express one or more subtypes of nucleotide receptor together with various combinations of the ecto-nucleotidases used for degrading and/or interconverting extracellular nucleotides (5). Recent studies using knockout mice that lack expression of particular nucleotide receptors or ecto-nucleotidases have suggested important *in vivo* roles for extracellular ATP or other nucleotides in a variety of inflammatory, nociceptive, hemostatic, and motility responses (6-12).

The physiological sources of the extracellular nucleotides that elicit these complex tissue responses remain largely uncharacterized. A major exception is the well-established ability of neurons, neuroendocrine cells, and platelets to release ATP via Ca^{2+}-regulated exocytosis of nucleotides compartmentalized within synaptic vesicles or dense core granules (13). However, many cell types that express nucleotide receptors lack direct physical proximity to neurons or degranulating platelets. Thus, identification of alternative sources of extracellular nucleotides, as well as elucidation of additional cellular mechanisms that underlie the release of nucleotides, are significant areas of current investigation (14). Because all cells contain ATP, all cell types are potential sources of extracellular ATP given appropriate physiological or pathological stimuli. Two recurring themes have emerged in recent studies of ATP release from cell types

other than neurons or platelets. First, intact cells constitutively release ATP at low rates by mechanisms that do not involve obvious lysis or loss of plasma membrane integrity (15, 16, 17). Second, the rate of non-lytic ATP release can be greatly increased by various extrinsic stimuli that result in perturbation of cell volume, shape, cytoskeletal organization, or intracellular Ca^{2+} homeostasis.

Several factors complicate or limit studies aimed at the direct quantitative evaluation of physiologically relevant ATP release. Cells express multiple ecto-nucleotidases that can rapidly hydrolyze ATP released at the extracellular surface (3, 4). Recent studies have indicated that ATP may also be synthesized from extracellular ADP via transphosphorylation reactions catalyzed by extracellular forms of nucleotide disphosphokinase (NDPK) or adenylate kinase (17-20). Although released or synthesized ATP will initially be spatially confined within unstirred layers at the cell surface, it will subsequently be diluted by diffusion and/or convection into the bulk extracellular volume. For these reasons, ATP concentrations at the extracellular surface will change rapidly and reflect a balance between the rates of release, hydrolysis, synthesis, and dilution into interstitial compartments (*in vivo*) or bathing media (*in vitro*). Most studies of ATP release have involved removal of samples from the bulk extracellular media bathing cultured cells or isolated tissues at selected timepoints following stimulation; this is followed by subsequent analysis of ATP or ATP-derived metabolites within these media samples (14-20). The ATP levels measured in such bulk extracellular media samples are likely to significantly underestimate the amount of ATP actually released at the cell surface, particularly in cells/tissues with substantial unstirred surface layers or high ecto-ATPase activities. For example, assays based on second

messenger accumulation in astrocytes and epithelial cells indicate that non-lytic mechanical stimuli trigger the release of ATP and other nucleotides in amounts sufficient for robust autocrine (or paracrine) activation of various G protein-coupled P2Y nucleotide receptors (15, 16, 17). However, the concentrations of nucleotide directly measured in the media bathing these stimulated cells are orders of magnitude lower than the concentrations required for threshold activation of known P2Y receptors. This suggests that nucleotide receptors and ecto-nucleotidases compete for a limited pool of endogenously released nucleotides within cell surface microenvironments that are functionally segregated from the bulk extracellular compartment.

To address this possibility, we have used luciferase-based methods to continuously record ATP levels in extracellular compartments of human 1321N1 astrocytoma cell monolayers under resting conditions, during activation of Ca^{2+}-mobilizing receptors, or during mechanical stimulation by hypotonic stress. Soluble luciferase was used as an indicator of ATP levels within the bulk extracellular compartment while a surface-adsorbed protein A-luciferase was employed as a spatially localized probe of ATP levels at the immediate cell surface. Significant accumulation of ATP in the bulk extracellular compartment, under either resting or stimulated conditions, was observed only when endogenous ecto-ATPase activity was pharmacologically inhibited. In contrast, accumulation of submicromolar ATP in the cell surface microenvironment was readily measured even in the absence of ecto-ATPase inhibition. This indicated that the spatially colocalized luciferase could effectively compete with endogenous ecto-ATPases for released ATP. Other experiments revealed a critical role for elevated cytosolic [Ca^{2+}] in the ATP release mechanism triggered by thrombin or

muscarinic receptors, but not in ATP release stimulated by hypotonic stress. Our observations indicate that ATP release sites are functionally colocalized with ecto-ATPases at the astrocyte cell surface. This co-localization may act to spatially restrict the actions of released ATP as a paracine or autocrine mediator of cell-to-cell signaling.

EXPERIMENTAL PROCEDURES

Reagents - Firefly luciferase ATP assay mix (FL-AAM), ATP standards (FL-AAS), luciferin (luciferase substrate), monoclonal anti-human CD14 antibody (Clone UCHM-1), potato apyrase (grade I), thrombin (from bovine plasma), carbachol, digitonin, and βγMeATP were from Sigma-Aldrich. A synthetic peptide (SFLLRD) that acts as a TRAP (Thrombin Receptor Activating Peptide) reagent was obtained from SynPep. Cell lysis assays were performed using the Boehringer Mannheim LDH assay kit. BAPTA-AM and fura2-AM were obtained from Molecular Probes. ProA-luciferase was purified from JM109 *Escherichia coli* cells transformed with pMALU5 plasmid DNA provided by Dr Eiry Kobatake (Tokyo Institute of Technology). CD14 cDNA in pcDNA3 was generously provided by Dr. Paul Godowski (Genentech). Wildtype 1321N1 human astrocytoma cells were obtained from Drs. Ken Harden and Jose Boyer (University of North Carolina – Chapel Hill).

***Cell Culture*.** 1321N1 human astrocytoma cells were maintained in Dulbecco's minimal essential medium (DMEM) containing 10% iron-supplemented bovine calf serum (Hyclone), penicillin (100 U/ml), and streptomycin (100 μg/ml). For some experiments, 1321N1 cells were transfected with human CD14 cDNA using Effectene reagent (Qiagen). Selection of cells that stably express CD14 was accomplished with G418 (500

μg/ml) added 48 hours after transfection. After 3 weeks of selection, the stably transfected cultures (1321N1-CD14) were maintained under continuous G418 selection. For all luciferase-based experiments, 1321N1 cells were seeded on 35-mm dishes (Falcon) at $3x10^5$ cells per dish. All experiments were conducted on confluent cell monolayers cultured for 5 to 7 days post plating such that each dish contained ~$1x10^6$ cells. Some experiments used 1321N1 cell suspensions (~$1x10^6$/ml) prepared by standard trypsin (0.05%) detachment procedures.

Assay of ATP levels in the bulk extracellular media compartment by soluble luciferase- An online luciferase-based protocol for measuring extracellular ATP levels in cultures of adherent cell monolayers was adapted from methods first developed by Schwiebert and colleagues (21, 22) and recently modified by our laboratory (23). All extracellular ATP measurements were performed using a Turner Designs (TD 20/20) luminometer capable of accommodating 35 mm culture dishes. Unless otherwise stated, 35 mm dishes with adherent cells were washed twice with 2 ml of basal saline solution (BSS) containing: 130 mM NaCl, 5 mM KCl, 1.5 mM $CaCl_2$, 1 mM $MgCl_2$, 25 mM Na.HEPES (pH 7.5), 5 mM glucose, and 0.1% bovine serum albumin (BSA). The washed monolayers were then bathed in 1 ml BSS and incubated for ~45 minutes at room temperature (22-24^{o}C), prior to experimental manipulation. Experiments were performed at room temperature using cell-free or cell-containing 35 mm dishes treated under identical assay conditions. Lyophilized firefly luciferase ATP assay mix (FL-AAM, Sigma) containing luciferase, luciferin, $MgSO_4$, dithiothreitol, EDTA, BSA, and Tricine buffer was reconstituted with 5 ml of sterile filtered water and stored in frozen 500 μl aliquots. For experiments, aliquots were thawed at room temperature and diluted 1:25 (40 μl) into the 35 mm dishes (±

adherent 1321N1 cells) containing 1 ml BSS immediately prior to start of luminescence recordings. ATP-dependent changes in extracellular luciferase activity were measured as relative light unit (RLU) values integrated over 5 second photon counting periods with dishes being gently stirred between readings. For most experiments, the luciferase activity was recorded every 1 or 2-minutes for up to 150 minutes. ATP contamination and possible effects of various test reagents on luciferase activity were assessed using cell-free 35 mm dishes under identical assay conditions. Calibration curves were generated for each experiment by addition of ATP standards (FL-AAS, Sigma) to cell-free dishes. Under these assay conditions, the limit of ATP detection was 100 pM (100 fmol/1 ml assay volume) and luminescence was linear with increasing ATP concentration to 1000 nM.

Ecto-ATPase assay **-** To assess the ecto-ATPase activity of 1321N1 cell monolayers under conditions used for the ATP release experiments, a pulse of 100 nM exogenous ATP was added to cell-free dishes or 1321N1 monolayers containing luciferase assay medium as described above. Decreases in ATP-dependent luminescence were recorded every 2 minutes for 20 minutes. Ecto-ATPase inhibition studies were performed using resting 1321N1 monolayers that were incubated with various concentrations of the poorly metabolizable analog βγ-methylene ATP (βγMeATP) 10 to 15 minutes prior to addition of the 100 nM ATP pulse.

ATP Release Stimuli **-** After extracellular luciferase activity reached steady state, 1321N1 cells were stimulated for up to 20 minutes with 2 U/ml thrombin (1 U/ml = 24 nM), 3 μM of the SFLLRD-TRAP, 100 μM carbachol, or hypotonic stress (a 30 % decrease in tonicity) in the absence or presence of βγMeATP (3 -300 μM). In some

experiments, thrombin was tested at concentrations ranging from 0.1 mU/ml (2.4 pM) up to 3 U/ml (72 nM) while SFLLRD-TRAP was varied from 30 nM through 10 μM. Luciferase activity was recorded every 1-2-minutes during the stimulation period. All additions to the 1 ml ATP assay volumes were made from 100- to 1000-fold concentrated stocks of the various test reagents. To stimulate cells by hypotonic stress, 405 μl of BSS was carefully replaced with 405 μl of an otherwise identical, luciferase-supplemented assay solution lacking only NaCl; this reduced the NaCl concentration of the extracellular assay medium from 130 mM to 77 mM. Control experiments involving replacement of 405 μl of assay solution with an equivalent volume of fresh, isotonic assay medium verified that this medium replacement protocol produced negligible mechanically-induced ATP release. Separate ATP calibrations were performed for the reduced NaCl assay medium to control for the known effects of Cl^- concentration on luciferase activity (51, 66). At the end of each assay, the cells were permeabilized with digitonin (50 μg/ml) to release cytosolic ATP as a measure of relative cell mass. Potato apyrase (5 U/ml) was used to scavenge released extracellular ATP and provide an index of background light production.

Assay of ATP levels in the extracellular surface microenvironment by cell-attached luciferase - Measurements of ATP in the cell surface microenvironment were performed by antibody-dependent adsorption of a protein A-luciferase chimeric protein (proA-luc) to the extracellular surface of intact 1321N1 cells. ProA-luc was expressed in bacteria as previously described (24). Briefly, pMALU5-transformed cultures of JM109 *Escherichia coli* were lysed by sonication in 150 mM NaCl, 100 mM Tris.HCl (pH 7.0), 5 mM EDTA, and 5 mM DTT supplemented with 200 μg/ml lysozyme and protease inhibitors.

The soluble lysate fraction containing recombinant protein A-luciferase (proA-luc) chimeric protein was filtered through 0.2 μm Acrodisks (Gelman Sciences), applied to a HiTrap desalting column (Pharmacia), and buffer exchanged into a minimal BSS lacking calcium, magnesium, glucose and BSA using FPLC (Fast protein liquid chromatography) protocols. The buffer-exchanged bacterial lysates were pooled, tested for luciferase activity, and stored as 1 ml aliquots at –80^{o}C. 35 mm culture dishes containing either 1321N1-CD14 or wild type 1321N1 cell monolayers were washed once with 2 ml BSS and incubated with gentle stirring for 1 hour at room temperature in 1 ml BSS containing 1 μg anti-CD14 antibody. Following removal of the primary antibody solution, the cell monolayers were washed once with 2 ml BSS, and then incubated with 1 ml of buffer-exchanged bacterial lysate containing undiluted proA-luc for 1 hour at room temperature with gentle stirring. The proA-luc solution was then aspirated and the cell monolayers were washed with 2 ml BSS. The cells were then re-equilibrated for ~30 minutes in 1ml fresh BSS at room temperature before being supplemented with 150 μM luciferin (2.5 μl of 60 mM stock/ml). ATP release was stimulated using 2 U/ml thrombin with and without βγMeATP (300 μM) to decrease ATP scavenging at the cell surface. ProA-luc activity was recorded every 12 seconds for up to 18 minutes. Control experiments on wild type 1321N1 versus 1321N1-CD14 cells incubated with and without anti-CD14 antibody verified that maximal proA-luc attachment was dependent on both CD14 expression and pre-incubation with anti-CD14 antibody. Calibration curves were generated by addition of exogenous ATP standards to anti-CD14 and proA-luc-coated 1321N1-CD14 cells.

Manipulation and measurement of intracellular Ca^{2+} concentration - The role of cytosolic [Ca^{2+}] in basal and stimulated ATP release was studied using either 1321N1 cell monolayers or suspensions as described above. 1321N1 cells were incubated with serum-free DMEM containing 0.1% BSA plus or minus the cell-permeable calcium chelator BAPTA-AM (1,2-bis (2-Aminophenoxy)ethane-N,N,N',N'-tetraacetic acid tetrakis acetoxymethyl ester) at 10 μM for 30 minutes at 37°C. BAPTA-loaded or mock-loaded 1321N1 monolayers were then used for luciferase-based assays of extracellular ATP exactly as described above. Suspended cells were prepared for measurements of intracellular Ca^{2+} concentration by incubation in BSS containing 1 μM fura2 acetoxymethyl ester (fura2-AM) at room temperature for 1 hour. The suspensions were washed twice with BSS before fura2 fluorescence (339-nm excitation and 500-nm emission) was measured and calibrated at 37°C in a stirred cuvette as previously described (25). The effects of thrombin, SFLLRD-TRAP, carbachol, or βγMeATP on intracellular Ca^{2+} were measured in parallel samples of BAPTA-loaded or non-BAPTA loaded cells.

Data Evaluation – Individual experimental manipulations were performed using duplicate or triplicate dishes of 1321N1 monolayers from the same cell passage. Integrated RLU recordings of luciferase activity were immediately downloaded into Microsoft Excel using the Turner Designs spreadsheet interface software (version 2.0.1, Sunnyvale, CA). RLU values were converted to ATP concentrations using calibration curves generated on the same day using identical assay solutions and conditions. Prism 3.0™ software (GraphPad) was used to compute the means and standard errors of the calculated ATP levels from identical, independent experiments that were repeated 2-7

times. For ecto-ATPase inhibition studies, Excel (Microsoft) was used to fit the decay of the exogenously added ATP bolus to an exponential curve. Rate constants (k) were then calculated for each curve fit. All experiments were repeated 2-7 times. Figures were generated using Prism 3.0^{TM} (GraphPad) and Illustrator 7.0 ^{TM} (Adobe) software.

RESULTS

Constitutive ATP release and extracellular metabolism by human 1321N1 astrocytes at steady state **---** Immediately after 35 mm dishes of 1321N1 monolayers were washed and transferred from tissue culture medium to the luciferase-supplemented assay medium, 50-70 nM ATP was present in the bulk 1 ml extracellular volume (Fig. 1A). This elevated extracellular ATP reflects release of endogenous ATP from the cells due to mechanical stimulation of poorly characterized ATP release pathways (15, 17). The ATP then rapidly decreased to ~2 nM within 20 minutes. Within 45-60 minutes after medium transfer, the extracellular ATP stabilized at a non-zero steady state of ~1 nM ATP that was 10-fold higher than the limit of ATP detection (100 pM) under these assay conditions. Addition of potato apyrase to the assay medium caused a rapid decrease in extracellular [ATP] to the limit of assay detection (not shown). The steady-state content of 1 pmol ATP measured in the 1 ml extracellular volume was equivalent to only 0.01-0.02 % of the total digitonin-releasable ATP (5-10 nmol) within the approximately 10^6 1321N1 cells that comprised each monolayer. Longer-term incubation of the monolayers for up to 100 minutes failed to decrease extracellular ATP levels to the assay detection limit. Addition of digitonin (as a plasma membrane permeabilizing agent) to cell-containing dishes, but not cell-free dishes, resulted in a rapid increase in bulk

extracellular [ATP] to ~5 μM. This provided a measure of total cytosolic ATP content and was consistent with a cytosolic concentration of 5 mM ATP being diluted 1000-fold into the 1 ml assay volume from the ~1 μl total intracellular volume of the 10^6 cells that comprise the 1321N1 monolayer.

When the monolayers were pulsed with 100 nM ATP after 100 minutes of equilibration, this exogenous ATP was degraded at a rate similar to that which characterized the scavenging of the ATP released from endogenous stores upon medium exchange (Fig. 1B). The ATP level decayed with a single exponential rate consistent with a *t½* of ~12-14 minutes. In contrast, when 100 nM ATP was added to cell-free plates containing identical luciferase assay medium, the ATP was degraded at a much slower rate reflecting the intrinsic pyrophosphatase activity of the luciferase used as the ATP sensor. In another study, we have developed the use of β,γ-methylene-ATP (βγMeATP) as an inhibitor of the ecto-ATPase(s) expressed by 1321N1 astrocytes (Joseph and Dubyak, unpublished observations). Those experiments indicated that βγMeATP could be used at millimolar concentrations with no confounding side-effects due to ATP contamination, inhibition of luciferase as an ATP sensor, or action as a nucleotide triphosphate substrate for ecto-nucleotide diphosphokinase (NDPK)-mediated phosphorylation of extracellular ADP (data not shown). Figure 1B shows that 300 μM βγMeATP markedly inhibited (by 95%) the ability of 1321N1 monolayers to rapidly scavenge a 100 nM pulse of exogenous ATP.

Effects of ecto-ATPase inhibition on steady-state ATP levels in the bulk extracellular medium ---

If the basal [ATP] within the bulk extracellular medium reflects a steady-state balance between constitutive ATP release and hydrolysis by ecto-ATPases, then acute inhibition of the ecto-ATPases should perturb this steady-state and result in an elevated level of extracellular ATP. Figure 2A illustrates how acute addition of 300 μM βγMeATP causes extracellular ATP to gradually increase to ~3 nM ATP over 20 minutes. In the absence of βγMeATP, extracellular ATP remained at the 1 nM steady-state level over this same time period. This slow accumulation of extracellular ATP induced by βγMeATP corresponded to an ATP release rate of ~0.1 pmol/min/10^6 cells. Because similar results were observed using monolayers that were not periodically agitated after addition of the βγMeATP (not shown), cell lysis was an unlikely cause for this slow accumulation of ATP in the bulk extracellular compartment. Identical experiments using cell-free dishes verified that the βγMeATP-mediated increase in ATP concentrations was dependent on the presence of 1321N1 monolayers and was not due to *de novo* synthesis of extracellular ATP as a consequence of contaminating adenylate kinase or nucleotide diphosphokinase activities in the luciferase assay medium. These results are consistent with previous observations by Lazarowksi et al. (17) who used isotopic equilibrium methods to demonstrate a steady-state balance between constitutive release of endogenous ATP from resting 1321N1 astrocytes and the degradation of that ATP by ecto-ATPases.

Thrombin-stimulated ATP release from 1321N1 astrocytes in the absence or presence of ecto-ATPase inhibition --- Previous studies have established that 1321N1 astrocytes express G protein-coupled protease-activated receptors (PAR1) for thrombin (26, 27). In

the absence of ecto-ATPase inhibition, stimulation of 1321N1 monolayers with thrombin resulted in only a transient 2-fold rise in bulk extracellular ATP to 2 nM within 2 minutes followed by a return to the baseline level over the next 10 minutes (Fig. 2A). This very modest and transient increase contrasted with the sustained 30- to 80- fold increase in bulk extracellular ATP observed when 1321N1 monolayers were simultaneously exposed to both thrombin and 300 μM βγMeATP as costimuli (Fig. 2B). The strongly synergistic action of thrombin and βγMeATP on accumulation of extracellular ATP indicates that ecto-ATPases can rapidly scavenge increased amounts of endogenous ATP released onto the cell surface in response to thrombin receptor activation. Moreover, the steadily maintained plateau in extracellular [ATP] throughout the 20-minute period after costimulation with βγMeATP and thrombin suggests that thrombin mobilizes a limited and slowly replenished pool of releasable ATP, such as exocytotic vesicles that sequester nucleotides. Increasing the βγMeATP in the costimulus from 3 μM to 300 μM at constant thrombin produced a concentration-dependent increase in the peak magnitude of the extracellular ATP detected by luciferase (Fig. 2B). Consistent with the partial inhibition of ecto-ATPase activity at βγMeATP < 300 μM (Joseph and Dubyak, unpublished observations), the increases in extracellular ATP were not steadily maintained when thrombin was applied as a costimulus with 3 or 30 μM βγMeATP.

Varying the thrombin concentration (0.0001 – 3000 mU/ml) at constant βγMeATP (300 μM) indicated that the threshold for thrombin-induced ATP release was in the 1 mU/ml (~20 pM) range (Figs. 3A and 3C). However, the concentration-response relationship describing thrombin-induced ATP accumulation was unusually steep with peak ATP accumulation at 10 mU/ml (240 pM) followed by modest decrease to a plateau

level of ATP release at $\geq$30 mU/ml thrombin. Although most acute actions of thrombin on cellular function can be ascribed to its proteolytic activation of PAR-family receptors, it was important to test whether thrombin might additionally potentiate extracellular ATP accumulation by proteolytic modification of other proteins directly involved in ATP release or extracellular ATP metabolism (28). Figs. 3B and 3D illustrate the rates and magnitudes of ATP accumulation observed in 1321N1 monolayers costimulated with βγMeATP plus various concentrations of the hexapeptide, SFLLRD, which acts as a reversible PAR1 agonist or TRAP reagent (Thrombin Receptor Activating Peptide). The maximal rates and peak magnitudes of SFLLRD-TRAP-induced ATP accumulation were similar to those observed when thrombin *per se* was used to activate PAR1. This suggested that the effects of thrombin on ATP release and accumulation are due solely to its proteolytic actions on PAR-family receptors. The EC_{50} of ~0.5 μM characterizing this action of SFLLRD-TRAP was similar to the EC_{50} for TRAP-induced Ca^{2+} mobilization in these cells (data not shown). As with thrombin, stimulation of 1321N1 monolayers with SFLLRD-TRAP (up to 10 μM) in the absence of βγMeATP induced only a small (3-4 nM peak) and transient accumulation of ATP within the bulk extracellular medium (data not shown).

Thrombin-stimulated release of ATP into the extracellular surface microenvironment -- Figs. 2 and 3 indicate that, in the absence of ecto-ATPase inhibition, most of the ATP released in response to thrombin or SFLLRD-TRAP is hydrolyzed before it can diffuse into the bulk extracellular compartment containing the soluble luciferase sensor. This suggests that ATP release and hydrolysis occurs in a cell surface microcompartment that

is functionally segregated from the bulk extracellular compartment. In a previous study, we demonstrated that a protein A-luciferase chimeric protein (proA-luc) could be localized to the extracellular surface of intact cells via high-affinity association between the protein A moiety and antibodies bound to extracellular epitopes of plasma membrane proteins (24). This effectively localizes and restricts the luciferase to the immediate extracellular surface. As schematically illustrated in Fig. 4, this may also facilitate targeting of the luciferase to plasma membrane subdomains containing the endogenous ecto-ATPases and thereby allow the luciferase-ATP sensor to effectively compete with ecto-nucleotidases for endogenous ATP as it is released onto the cell surface. To localize proA-luc to the surface of 1321N1 cells, we generated sublines (1321N1-CD14) that were stably transfected with an expression plasmid encoding human CD14. CD14 is a GPI-anchored plasma membrane protein, normally expressed only in myeloid leukocytes, that acts as a cell surface binding site for endotoxin/lipopolysaccharide (29). Immunofluorescence microscopy using a monoclonal anti-human CD14 antibody verified cell surface expression of CD14 in the 1321N1-CD14 lines but not in the wildtype parental 1321N1 cells (data not shown). This same monoclonal antibody was used to specifically adsorb the proA-luc chimeric protein to the extracellular surface of 1321N1-CD14 monolayers. ProA-luc attachment was strongly CD14-dependent because calibrations with ATP standards revealed 30-fold higher RLU values from proA-luc-coated 1321N1-CD14 cells compared to wild type 1321N1 monolayers that were subjected to identical incubations with anti-CD14 and proA-luc (Table 1). In the absence of the anti-CD14 precoating, similar low levels of non-specifically adsorbed proA-luc were observed with wildtype 1321N1 and 1321N1-CD14 monolayers (not shown). The

limit of detection for ATP (added to the bulk extracellular compartment) was in the 10-30 nM range (Table 1).

Fig. 5 compares the timecourses of thrombin-induced ATP release from 1321N1-CD14 monolayers using either the previously described soluble luciferase protocol or the cell-attached proA-luc method; panels A and B illustrate the results obtained using two different subclones of CD14-transfected 1321N1 cells. To assess the early kinetics of the ATP release process, luminescence was recorded at 12-second intervals in the absence or and presence of 300 μM βγMeATP. When assayed by the soluble luciferase protocol, the thrombin-induced ATP release responses in 1321N1-CD14 cells were similar to those observed with wildtype cells, i.e. transient accumulation of extracellular ATP in the absence of ecto-ATPase inhibition versus a strongly synergistic response to thrombin and βγMeATP added as costimuli. Thrombin activation of these particular 1321N1 sublines in the absence of βγMeATP caused bulk ATP levels to transiently increase by ~15 nM within 3 minutes (Figs. 5A and B), corresponding to an initial release rate of ~5 pmol/min/10^6 cells. This response was higher than was observed with the wildtype 1321N1 monolayers illustrated in Fig. 2A and may indicate either increased expression of the ATP release machinery in the clonally selected sublines or an elevated rate of ATP diffusion into the bulk phase medium due to increased mixing that accompanied the 10-fold higher frequency of luminescence readings (every 12 seconds versus every 2 minutes).

Significantly, when cell-attached luciferase was used as the ATP sensor, thrombin stimulation alone was sufficient to trigger rapid accumulation of ATP at the extracellular surface to peak concentrations in the 100-300 nM range (Figs. 5A and 5B). This

corresponded to an initial release rate of >100 pmol ATP/min/10^6 cells which is at least 20-fold higher than was observed using soluble luciferase as the ATP sensor. The cell surface ATP concentration reached a peak within 1 minute after thrombin addition and was then maintained at a plateau for another 60-90 seconds before decaying toward baseline levels over the next 5 minutes. When thrombin was delivered as a costimulus with βγMeATP, the increasing phase of ATP accumulation was prolonged to 2 minutes resulting in peak cell surface levels 1.5- to 1.8-fold higher (150-550 nM) than was observed in the absence of βγMeATP. The presence of βγMeATP also affected decay kinetics of the cell surface ATP signal. The plateau was maintained for only 20 seconds and ATP levels did not return to basal levels, but instead remained elevated at the 50 - 150 nM range. Although much of the ATP released onto the cell surface during thrombin stimulation may diffuse into, and be diluted within the bulk medium compartment, ecto-ATPase inhibition clearly facilitates the further accumulation of ATP at the cell surface.

Carbachol-stimulated ATP release from 1321N1 astrocytes in the absence or presence of ecto-ATPase inhibition – To test whether agonists for other G-protein coupled receptors could mimic the effects of thrombin or SFLLRD-TRAP on ATP release, similar experiments were performed using 100 μM carbachol to maximally activate the M1-muscarinic receptors that have been previously characterized in 1321N1 astrocytes (26). Figure 6 shows that carbachol alone triggered only minor and transient accumulation of extracellular ATP (2 nM peak at 4 minutes) in the bulk medium compartment of 1321N1 monolayers. As observed with thrombin, carbachol acted synergistically with βγMeATP (added as a costimulus) to trigger accumulation of ~12 nM extracellular ATP within 5

minutes. However, both the initial rate of ATP release and the maximal plateau level of accumulated ATP in these carabachol-stimulated cells were invariably 3- to 5-fold lower than measured in parallel 1321N1 monolayers (same passage assayed on the same day) stimulated with thrombin or SFLLRD-TRAP (see also Fig. 9).

Hypotonic stress-stimulated ATP release from 1321N1 astrocytes in the absence or presence of ecto-ATPase inhibition – Multiple cell types have been shown to release nucleotides when subjected to hypotonic stress as part of a regulatory volume decrease response to osmotic swelling (22, 30-35). 1321N1 monolayers challenged with a 30% decrease in tonicity accumulated 3 nM ATP in the bulk extracellular compartment over a 10-minute period. However, induction of hypotonic stress as a co-stimulus with βγMeATP resulted in a sustained rise in extracellular ATP to ~60 nM over a 20 min test period (Fig. 7). This result indicates that ATP released in response to either activated G protein-coupled receptors or mechanical stimulation can be catabolized with similar efficiency in extracellular compartments at the 1321N1 cell surface before dilution into the bulk extracellular fluid phase. Although the magnitude of the hypotonicity-induced ATP accumulation was similar to that triggered by thrombin receptor activation, the rate of the ATP accumulation was at least 5-fold slower with the hypotonic stimulus. This suggests that the two stimuli may target mechanistically distinct ATP release pathways.

Role of cytosolic Ca^{2+} in basal and stimulated ATP release from 1321N1 astrocytes – In platelets, thrombin activates Gq-coupled PAR1 receptors to trigger the Ca^{2+}-dependent exocytosis of ATP-containing dense granules (28). Given that the PAR1 and M1

receptors expressed in 1321N1 astrocytes also activate PI-PLCβ and mobilization of IP_3-sensitive Ca^{2+} stores, we tested the possible role of cytosolic Ca^{2+} as a regulator of ATP release. The basal cytosolic [Ca^{2+}] in 1321N1 cells was ~200 nM (Fig. 8). Thrombin and carbachol both rapidly triggered transient increases in [Ca^{2+}] that peaked in the 2 μM range (Figure 8A). However, the response to carbachol was sustained for several minutes in contrast to the rapid decay within 60 seconds of the thrombin-induced Ca^{2+} transient. When βγMeATP was tested at the 300 μM concentration routinely used to inhibit ecto-ATPase activity, a transient increase in [Ca^{2+}] to ~300 nM was also observed in some (e.g., Fig. 8A) but not all preparations of 1321N1 astrocytes. 1321N1 cells lack significant expression of the known Gq-coupled P2Y nucleotide receptor subtypes (P2Y1, P2Y2, P2Y4, P2Y6, and P2Y11) and βγMeATP is a poor agonist for those receptor subtypes (1, 5, 15). Although βγMeATP can also act as an agonist for certain P2X receptors (1), 1321N1 cells lack expression of any of the seven known P2X subtypes (67). Thus, the underlying mechanism for this modest and variable βγMeATP-induced Ca^{2+} transient is unclear. As expected, the ability of carbachol, thrombin, or βγMeATP to trigger transient increases in cytosolic [Ca^{2+}] was completely ablated in parallel samples of 1321N1 cells that were loaded with the intracellular Ca^{2+}-chelator BAPTA (Fig 8B).

Basal and stimulated ATP release were then compared in control versus BAPTA-AM-loaded 1321N1 monolayers assayed in the presence of 300 μM βγMeATP to inhibit ecto-ATPase activity. Figure 9A shows that the slow rate of basal ATP release observed upon acute addition of βγMeATP was similar in the control and BAPTA-loaded cells. However, BAPTA-loading significantly (~75% inhibition) attenuated the rate and extent of ATP release triggered by thrombin and completely abrogated the carbachol-stimulated

ATP release (Figs 9B and 9C). These experiments also highlight the 4-fold larger magnitude of the ATP release triggered by thrombin versus carbachol despite the more sustained Ca^{2+} transients elicited by the latter agonist. The results suggest that increased cytosolic [Ca^{2+}] is an important signal for activation of the ATP release machinery by Gq-coupled receptors, but that thrombin additionally elicits ATP release via signaling pathways that do not require elevated Ca^{2+}. An involvement of Ca^{2+}-independent signaling pathways in ATP release was further supported by the inability of BAPTA-loading to substantially attenuate the accumulation of extracellular ATP in 1321N1 cells subjected to hypotonic stress (Fig. 9D).

Additive effects of thrombin receptor activation and hypotonic stress on ATP release from 1321N1 astrocytes – The markedly different consequences of BAPTA-loading on thrombin-induced ATP release versus hypotonicity-induced ATP release suggested that these stimuli trigger mechanistically distinct pathways of nucleotide export. This was tested by comparing the ATP release responses (in the presence of βγMeATP) to costimulation by simultaneous hypotonic stress and thrombin treatment versus stimulation by hyptonicity alone or thrombin alone (Fig. 10). Significantly, the costimulation protocol induced strictly additive effects on net ATP accumulation with regard to both time course and magnitude. Such additive actions are consistent with the possibility that 1321N1 astrocytes may release ATP (and perhaps other nucleotides) by parallel, non-interacting mechanisms.

DISCUSSION

Accumulation of ATP within a particular extracellular compartment will reflect both the rate of ATP release into that compartment from intracellular pools and the rate of ATP hydrolysis by locally expressed ectonucleotidases. This study provides several novel insights regarding the dynamics and regulation of extracellular ATP accumulation in a non-excitatory cell type, the 1321N1 human astrocytoma line. Stimulation of these cells with Ca^{2+}-mobilizing agonists for two different Gq-coupled receptors (PAR1 and M1-muscarinic) resulted in only minor increases in ATP levels within the bulk extracellular medium even at early time points following receptor activation. This contrasted with the rapid elevation of extracellular ATP to submicromolar levels at the immediate cell surface during PAR1 activation of 1321N1 cells in which the luciferase ATP sensor was tethered to a GPI-anchored plasma membrane protein. This result suggests that the PAR1-elicited ATP release is initially directed into an extracellular subcompartment that lacks rapid diffusional exchange with the extracellular medium bathing these astrocyte monolayers. As a result, much of the released ATP can be efficiently metabolized by ecto-ATPases that are present within – and possibly localized to – that same extracellular subcompartment prior to diffusion into the bulk extracellular fluid phase. This interpretation is further supported by pharmacological experiments that used high concentrations of an exogenous, poorly hydrolyzable ATP analog (βγMeATP) to competitively inhibit hydrolysis of the released ATP by the ecto-ATPases within the putative cell surface subcompartment. This repression of localized ATP scavenging readily facilitated diffusional equilibration of the released ATP with the bulk extracellular

fluid volume where it could be registered by the soluble luciferase ATP sensor. Taken together, the results of the tethered luciferase assays and the pharmacological experiments suggest that the sites of initial ATP release are focussed within plasma membrane subdomains characterized by high levels of local ecto-ATPase activity.

This apparent functional segregation of the immediate ATP release sites from the bulk extracellular compartment may involve spatial colocalization of the ATP release sites and ectonucleotidases within plasma membrane subdomains, such as caveolae or lipid raft-based invaginations, that enclose physically constrained extracellular spaces and thereby retard rapid exchange with the bulk extracellular space. The ability of the CD14-tethered luciferase to effectively monitor significant thrombin-induced ATP release even in the absence of βγMeATP indicates that CD14 acts to concentrate the cell surface luciferase ATP sensor to levels sufficient for effective competition with local ecto-ATPases. GPI-anchored proteins such as CD14 are often localized to lipid raft domains of the plasma membrane (36). Significantly, various purinergic signaling elements, including receptors (37, 38) and ecto-nucleotidases (39-41) have also been localized to raft domains and/or caveolae. Most germane to our observations is the finding by Robson and colleagues that the CD39 ecto-apyrase/ eNTDPase-1, the prototype of the ecto-NTDPase family, is localized to the caveolae of human endothelial cells (40). This caveolar association of CD39 was found to be dependent on post-translational modification by N-terminal palmitoylation (41).

It remains to be determined whether CD39 or another ecto-nucleotidase is the predominant βγMeATP-sensitive ecto-ATPase expressed in 1321N1 human astrocytes. The mammalian CD39 family of eNTDPases comprises six unique gene products that

encode intrinsic membrane proteins with two membrane-spanning domains, intracellular amino- and carboxy termini, and a large connecting loop that contains the catalytic activity (3, 4). Three of these family members (CD39/ eNTDPase-1, CD39-L1/ eNTDPase-2, and CD39-L3/ eNTDPase-4) function as plasma membrane-localized ecto-ATDPases that can hydrolyze extracellular ATP and/or ADP to AMP. These enzymes also metabolize other nucleotide tri- and diphosphates, including UTP and UDP, which are agonists for several P2Y receptor subtypes. Lazarowksi and colleagues have previously reported that 1321N1 cells express a significant ecto-NTPase activity that can metabolize both ATP and UTP (15, 17). These investigators also observed that 1321N1 cells additionally express robust ecto-nucleotide pyrophosphatase (eNPP) and ecto-nucleotide diphosphokinase (eNDPK) activities. The mammalian eNPP family includes three unique gene products that are class 2-type plasma membrane proteins (42). In rat C6 glioma cells (43, 44) and *Xenopus* oocytes (45), eNPP enzymes can hydrolyze βγMeATP to directly generate AMP which is subsequently metabolized to adenosine via the CD73 ecto-5'-nucleotidase. Extracellular NDPK (17-19) or ecto-adenylate kinase activities (20) add yet another complication to analyses of extracellular ATP accumulation because they can catalyze the extracellular synthesis ATP from ambient ADP in the presence of released or added nucleotide triphosphates. However, due to the methylene bridge between its β- and γ-phosphates, βγMeATP cannot act as a phosphate donor for NDPK-catalyzed phosphorylation of ADP (Joseph and Dubyak, unpublished observations).

Depending on the cell type and extrinsic stimulus, ATP can be released to extracellular compartments either by exocytosis of ATP-containing vesicles/granules or

by the facilitated efflux of cytosolic ATP through channels or transporters that can accommodate the size and charge of nucleotides. Our comparative analyses of ATP release from 1321N1 astrocytes stimulated by Gq-coupled receptor agonists versus hypotonic stress suggest that these cells express two (or more) parallel mechanisms for nucleotide export that are regulated by distinct signaling pathways. Given the strong inhibitory effect of BAPTA loading on ATP release induced by the Ca^{2+}-mobilizing PAR1 or M1 agonists, but not on ATP release elicited by hypotonicity, it is plausible to speculate that thrombin and carbachol primarily activate Ca^{2+}-dependent exocytosis of ATP-containing vesicles, while osmotic or mechanical stress may gate the Ca^{2+}-independent opening of ATP-conductive channels. However, it is also possible that increased Ca^{2+} may act to stimulate the gating of other ATP-permeable channels.

The best characterized analyses of exocytotic ATP secretion have utilized specialized secretory cells, such as chromaffin cells (46), PC12 cells (47) and platelets (24, 48), that compartmentalize ATP to submolar concentrations within dense core granules which can be easily identified by morphological criteria and biochemically isolated by standard cell fractionation (13). However, recent studies have suggested that exocytosis may be partially or fully responsible for the stimulus-induced release of ATP observed in multiple cell types, including astrocytes, that lack large numbers of specialized granules or vesicles known to contain ATP (49-51). It should be noted that even vesicles involved in the constitutive release of secreted proteins contain low levels of nucleotides due to important roles for intravesicular, nucleotide-dependent enzymes that catalyze covalent modification and maturation of secreted proteins (52). The studies of Maroto and Hamill (50) on ATP externalization from single *Xenopus* oocytes

suggested that brefeldin A-sensitive exocytotic pathways were involved in both basal and mechanically stimulated nucleotide release in that cell type. Some recent studies suggest that astrocytes and related glial-type cells may compartmentalize ATP in vesicles that can be released via regulated exocytosis. Using subcellular fractionation methods, Maienschein et al. (53) observed that primary rat astroglial cells contain ATP-enriched vesicles that colocalize with multiple proteins (synaptotagmin-I, synaptobrevin-II, SNAP25) implicated in regulated exocytosis. Coco et al. (51) have reported that mechanical stimulation or pharmacological agonists (phorbol esters) induced a release of ATP from primary neonatal rat astrocytes that could be partially blocked by bafilomycin, an inhibitor of the vesicular H^+-ATPases that set up the proton electrochemical gradients required for active accumulation of neurotransmitters, or tetanus toxin, which protelytically inactivates the V-SNARE, synaptobrevin-II.

In addition to regulated exocytosis, there is compelling evidence for the involvement of nucleotide-permeable channels in the release of ATP from various cell types, including astrocytes (54-56). Because cells contain millimolar levels of negatively charged $MgATP^{2-}$ within the cytoplasm and also maintain negative membrane potentials, there is a large electrochemical gradient for ATP efflux across the plasma membrane. Given this favorable electrochemical driving force, even brief activation of a nucleotide-permeable transporter could rapidly increase the rate of ATP delivery to local extracellular compartments. An involvement of channels as conduits for facilitated ATP efflux has been supported by two distinct but complementary experimental approaches. One is the direct electrophysiological measurement of membrane currents or channels for which ATP can act as an apparent charge carrier (32, 34, 57, 58). The other analysis is

based on the inhibition of ATP release by pharmacological agents known to target particular ion channels or classes of ion channels (30, 31, 33, 35, 57, 68). Based on these approaches, three classes of channels have been implicated in ATP release: 1) ATP-binding cassette (ABC) transporters (58); 2) volume-regulated anion channels or VRAC (32, 34); and 3) connexin hemichannels (54-56, 68). Whether one or more of these channels contributes to the ATP release observed in our 1321N1 astrocyte model system remains an open question.

Connexin hemichannels, which represent hexameric complexes of connexin subunits at non-junctional plasma membrane sites (59), have been particularly associated with ATP release from primary rat astrocytes subjected to metabolic inhibition (60) or direct mechanical stress (55, 56). In addition, Braet et al. (68) have recently observed that photoliberation of caged IP_3 (1,4,5-inositol trisphosphate) in endothelial cells triggered a Ca^{2+}-dependent release of ATP that was markedly repressed by peptide inhibitors of connexin hemichannels. Such hemichannels are appealing candidates as ATP efflux proteins given the known ability of some connexin-based gap junctions, which represent dodecameric complexes of connexin subunits at junctional plasma membrane loci, to directly mediate the cell-to-cell movement of nucleotides between junctionally-coupled cells. It is important to note that Nedergaard and colleagues (54, 55) have observed that BAPTA-loading represses the mechanically-induced ATP release that is correlated with gating of connexin-hemichannels in rat astrocytes. This contrasts with the BAPTA-insensitivity of the hypotonicity-stimulated ATP release we observed in the 1321N1 astrocytes. Alternatively, Hisadome et al. (32) have noted that the hypotonicity-induced ATP release associated with activated VRAC currents in bovine aortic endothelial cells

(BAEC) can occur in the absence of elevated cytosolic Ca^{2+}. Using the same BAEC model system and hypotonic stimuli, Koyama et al. (31) reported that ATP release was significantly inhibited by a pharmacological inhibitor (Y-27632) of the ROCK-I or ROCK-II Rho-activated kinases, as well as by botulinum C3 exotoxin which acts to inhibit activation of Rho-family GTPases. In preliminary experiments, we have failed to observe similar inhibitory effects of Y-27632 on the ATP release triggered by hypotonic stress (or PAR1 activation) in 1321N1 astrocytes. Thus, the nature or identity of candidate ATP-permeable channels that may contribute to nucleotide release from this latter cell model remains unclear at present. The possiblity that a single cell type, such as a 1321N1 astrocyte, may release ATP via parallel, non-cytolytic mechanisms involving both exocytosis and facilitated efflux through a nucleotide-permeable channel transporter is supported by a recent analysis of hypertonicity-induced ATP release from single *Xenopus* oocytes (61).

Regardless of the mechanism(s) that underlie ATP release from astrocytes, a growing body of data indicates that nucleotide release plays important autocrine and paracrine signaling roles in several known functions of astrocytes as modulators of neuronal function and survival in the central nervous system (62-65). The released ATP can act directly on ionotropic P2X receptors or certain G protein-coupled P2Y receptor subtypes that are expressed on astrocytes *per se* and adjacent neurons (both pre- and post-syntaptic). In conjunction with ecto-nucleotidase cascades, the released ATP also serves as an extracellular reservoir for the generation of the ADP or adenosine agonists that subsequently target yet other G protein-coupled receptors. One of the more intensively studied roles of local ATP release and P2 receptor activation in astrocyte function is the

intercellular propagation of Ca^{2+} waves among astrocytes or between astrocytes and neurons (54-56, 65). This intercellular propagation of signals that control a critical intracellular second messenger provides a rapid mechanism for coordinating the metabolic and electrical responses of local CNS regions to physiological changes in activity or pathological stresses, such as ischemia, mechanical trauma, or excitotoxicity. Although direct communication of Ca^{2+} waves via gap junction channels among physically adjacent astrocytes provides one mechanism, the release of ATP followed by the activation of Ca^{2+}-mobilizing P2Y receptors comprises a second pathway that does not require direct physical contact. In turn, the increase in astrocyte Ca^{2+} initiated by the activated P2Y receptors can induce the release of additional paracrine factors such as glutamate, prostaglandins, or other nucleotides, which act to further reinforce and coordinate the local response to the stress that initiated release of the ATP.

REFERENCES

1. North R.A. (2002) *Physiol. Rev*. **82**,1013-1067.
2. Abbracchio, M.P., Boeynaems. J-M., Barnard, E.A., Boyer, J.L., Kennedy, C., Miras-Portugal, M.T., King, B.F., Gachet, C., Jacobson, K.A., Weisman, G.A., and Burnstock, G. (2003) *Trends Pharmacol. Sci.*, **24**, 52-55
3. Zimmermann, H. (1999) *Trends Pharmacol. Sci.* **20,** 231-236,
4. Zimmermann, H. (2000) *Naunyn-Schmiedeberg's Arch. Pharmacol.* **362**, 299-309.
5. Ralevic, V. and Burnstock, G. (1998) *Pharmacol. Rev*. **50,** 413-492.
6. Fabre, J.E., Nguyen, M., Latour, A., Keifer, J.A., Audoly, L.P., Coffman, T.M., and Koller, B.H. (1999) *Nature Med*. **5**,1199-1202.
7. Cressman, V.L., Lazarowski, E.R., Homolya, L., Boucher, R.C, Koller, B.H., and Grubb, B.R. (1999) *J. Biol. Chem.* **274**, 26461-26468.
8. Robaye, B., Ghanem, E., Wilkin, F., Fokan, D., Van Driessche, W., Schurmans, S., Boeynaems, J-M., and Beauwens, R. (2003) *Mol. Pharmacol.* **63**, 777-783.
9. Mulryan, K., Gitterman, D.P., Lewis, C.J., Vial, C., Leckie, B.J., Cobb, A.L., Brown, J.E., Conley, E.C., Buell, G, Pritchard, C.A., and Evans, R.J. (2000) *Nature* **403**, 86-89.
10. Zhong, Y., Dunn, P.M., Bardini, M., Ford, A.P., Cockayne, D.A., and Burnstock, G. (2001) *Eur. J. Neurosci.* 14:1784-1792.
11. Labasi, J.M., Petrushova, N., Donovan, C., McCurdy, S., Lira, P., Payette, MM., Brissette, W., Wicks, J.R., Audoly, L., and Gabel, C.A.. (2002) *J. Immunol.* **168**, 6436-6445.

12. Enjyoji, K., Sevigny, J., Lin, Y., Frenette, P.S., Christie, P.D., Esch, J.S., 2nd, Imai, M., Edelberg, J.M., Rayburn, H., Lech, M., Beeler, D.L., Csizmadia, E., Wagner, D.D., Robson, S.C., Rosenberg, R.D. (1999) *Nature Med*. **5**, 1010-1017.

13. Unsworth, C.D. and Johnson, R.J. (1990) *Annals N.Y. Acad. Sci.* 603**,** 353-365**.**

14. Schwiebert, E.M. (1999) *Am. J. Physiol.* **276**, C1-C8.

15. Lazarowski, E.R., Homolya, L. Boucher, R.C., and Harden, T.K. (1997) *J. Biol. Chem*. **272,** 24348-24354.

16. Ostrom, R.S., Gregorian, C., and Insel. P.A. (2000) *J. Biol. Chem*. **275,** 11735-11739.

17. Lazarowski, E.R., Boucher, R.C., and Harden, T.K. (2000) *J. Biol. Chem*. **275**, 31061-31068.

18. Buxton, I.L., Kaiser, R.A., Oxhorn, B.C., and Cheek, D.J. (2001) *Am. J. Physiol. Heart Circ. Physiol.* **281,** H1657-1666.

19. Picher, M. and Boucher, R.C. (2003) *J. Biol. Chem*. Jan 27 [epub ahead of print]

20. Yegutkin, G.G., Henttinen, T., Samburski, S.S., Spychala, J., and Jalkanen, S. (2002) *Biochem*. *J*. **367**, 121-128.

21. Taylor, A.L., Kudlow, B.A., Marrs, K.L., Greunert, D.C., Guggino, W.B., and Schwiebert, E.M. (1998) *Am. J. Physiol. Cell Physiol.* **275**, C1391-C1406.

22. Schwiebert, L.M., Rice, W.C., Kudlow, B.A., Taylor, A.L., and Schwiebert, E.M. (2002) *Am. J .Physiol. Cell Physiol.* **282,** C289-C301.

23. Beigi, R. and Dubyak, G.R. (2000) *J. Immunol*. **165**, 7189-7198.

24. Beigi, R., Kobatake, E., Aizawa, M., and Dubyak, G.R. (1999) *Am. J.. Physiol. Cell Physiol.* **276**, C267-278.

25. Dubyak, G.R., Cowen, D.S., and Meuller, L.M. (1988) *J. Biol. Chem.* **263**, 18108-18117.

26. Majumdar, M., Seasholtz, T.M., Goldstein, D., de Lanerolle, P., and Brown, J.H. (1998) *J. Biol. Chem.* **273**, 10099-10106.

27. Post, G.R., Collins, L.R., Kennedy, E.D., Moskowitz, S.A., Aragay, A.M., Goldstein, D., and Brown, J.H. (1996) *Mol. Biol. Cell*. **7**, 1679-1690.

28. Macfarlane, S.R., Seatter, M.J., Kanke, T., Hunter, G.D., and Plevin, R. (2001) *Pharmacol. Rev*. **53,** 245-282.

29. Triantafilou, M., and Triantafilou, K. (2002) *Trends Immunol*. **23**, 301-314.

30. Feranchak , A.P., Roman, R.M., Doctor, R.B., Salter, K.D., Toker, A., and Fitz, J.G. (1999) *J. Biol. Chem*. **274,** 30979-30986.

31. Koyama, T., Oike, M., and Ito, Y. (2001) *J. Physiol.* **532**, 759-769.

32. Hisadome, K., Koyama, T., Kimura, C., Droogman, G., Ito, Y., and Oike M. (2002) *J. Gen. Physiol*. **119**, 511-520.

33. Hazama, A., Shimizu, T., Ando-Akatsuka, Y., Hayaski, S., Tanaka, S., Maeno, E., and Okada, Y. (1999) *J. Gen. Physiol.* **114**, 525-533.

34. Sabirov, R.Z., Dutta, A.K., and Okada, Y. *J. Gen. Physiol*. **118**, 251-266.

35. Hazama, A., Fan, H-T., Abdullaev, I., Maeno, E., Tanaka, S., Ando-Akatsuka Y., and Okada, Y. (2000) *J.Physiol*. **523**, 1-11.

36. Brown, D.A. and London, E. (2000) *J. Biol. Chem.* **275**, 17221-17224.

37. Lasley, R.D., Narayan, P., Uittenbogaard, A., and Smart, E.J. (2000) *J. Bio.l Chem*. **275,** 4417-4421.

38. Kaiser, R.A., Oxhorn, B.C., Andrews, G., and Buxton, I.L. (2002) *Circ. Res*. **91**, 292-299.

39. Misumi, Y., Ogata, S., Hirose, S., and Ikehara, Y. (1990) *J. Biol. Chem*..**265,** 2178-2183.

40. Kittel, A., Kaczmarek, E., Sevigny, J., Lengyel, K., Csizmadia, E., and Robson, S.C. (1999) *Biochem*. *Biophys. Res. Commun.* **262**, 596-599

41. Koziak, K., Kaczmarek, E., Kittel, A., Sevigny, J., Blusztajn, J.K., Schulte Am Esch, J. 2nd, Imai, M., Guckelberger, O., Goepfert, C., Qawi, I., and Robson, S.C. (2000) *J Biol Chem*. 275:2057-62. 2000

42. Bollen, M., Gijsbers, R., Ceulemans, H., Stalmans, W., and Stefan, C. (2000*) Crit. Rev. Biochem. Mol. Biol.* **35,** 393-432.

43. Grobben, B., Anciaux, K., Roymans, D., Stefan, C., Bollen, M., Esmans, E.L., and Slegers, H. (1999) *J. Neurochem*. **72**, 826-834.

44. Ohkubo, S., Kumazawa, K., Sagawa, K., Kimura, J., and Matsuoka, I. (2001) *J. Neurochem*. **76**, 872-880.

45. Matsuoka, I., Ohkubo, S., Kimura, J., and Uezono, Y. (2002) *Mol. Pharmacol*. **61**, 606-613.

46. Rojas, E., Pollard, H.B., and Heldman, E**.** (1985) *FEBS Lett.* **185**, 323-327.

47. Kasai, Y., Ohta, T., Nakazato, Y., and Ito, S. (2001) *J. Vet. Med. Sci*. **63**, 367-372.

48. Siess, W**.** (1989) *Physiol. Rev*. **69**, 58-178.

49. Bodin, P., and Burnstock, G. (2001) J. *Cardiovasc. Pharmacol*. **38**, 900-908.

50. Coco, S., Calegar,i F., Pravettoni, E., Pozzi, D., Taverna, E., Rosa, P., Matteolim M., and Verderio, C. (2003) *J. Biol. Chem*. **278**, 1354-1362.

51. Maroto, R. and Hamill, O.P. (2001) *J. Biol. Chem.* **276**, 23867-23872.

52. Hirschberg C.B., Robbins, P.W., and Abeijon, C. (1998) *Ann. Rev. Biochem.* **67**, 49-69.

53. Maienschein, V., Marxen, M., Volknandt, W., and Zimmermann, H. (1999) *Glia* **26**, 233-244.

54. Cotrina, M.L., Lin, J.H., Alves-Rodrigues, A., Liu, S., Li, J., Azmi-Ghadimi, H., Kang, J., Naus, C.C., and Nedergaard, M. (1998). *Proc. Natl. Acad. Sci. U S A.* **95**, 15735-15740.

55. Arcuino, G., Lin, J.H., Takano, T., Liu C, Jiang, L., Gao, Q., Kang, J., and Nedergaard, M. (2002) *Proc. Natl. Acad. Sci. U S A.* **99**, 9840-9845.

56. Stout, C.E., Constantin J.L., Naus, C.C.G., and Charles, A.C. (2002) *J. Biol. Chem*. **277**, 10482-10488.

57. Braunstein, G.M., Roman, R.M., Clancy, J.P., Kudlow, B.A., Taylor, A.L., Shylonsky, V.G., Jovov, B., Peter, K., Jilling, T., Ismailov, I.I., Benos, D.J., Schwiebert L.M., Fitz, J.G., and Schwiebert, E.M.. (2001) *J. Biol. Chem*. **276**, 6621-6630.

58. Reisen, I.L., Prat, A.G., Abraham, E.H., Amara, J.F., Gregory, R.J., Ausiello, D.A., and Cantiello, H.F. (1994) *J. Biol. Chem.* **269**, 20584-20591.

59. Li, H., Liu, T.F., Lazrak, A., Peracchia, C., Goldberg, G.S., Lampe, P.D., and Johnson, R.G. (1996) *J. Cell Biol.* **134**, 1019-1030.

60. Contreras, J.E., Sanchez, H.A., Eugenin, E.A., Speide,l D., Theis, M., Willecke, K., Bukauskas, F.F., Bennett, M.V., and Saez, J.C. (2002) *Proc. Natl. Acad. Sci. U S A.* **99**, 495-500.

61. Aleu, J., Martin-Satue, M., Navarro, P., Lara, I.P., Bahima, L., Marsal, J., and Solsona, C. (2003) *J. Physiol*. **547,** 209-219.

62. Ciccarelli, R., Ballerini, P., Sabatino, G., Rathbone, M.P., D'Onofrio, M., Caciagli, F., and Di Iorio, P. (2001) *Int. J. Dev. Neurosci*. **19**, 395-414.

63. Stevens, B. and Fields, R.D. (2000) *Science* **287**, 2267-2271.

64. Queiroz, G., Meyer, D.K., Meyer, A., Starke, K, and von Kugelgen, I. (1999) *Neuroscience* **91**, 1171-1181.

65. Scemes, E., Suadicani, S.O., and Spray, D.C. (2000) *J. Neurosci.* **20**, 1435-1445.

66. Denburg, J.L. and McElroy, W.D. (1970) *Arch. Biochem. Biophys.* **114**, 668-675.

67. Bianchi, B.R., Lynch, K.J., Touma, E., Niforatos, W., Burgard, E.C., Alexander, K.M., Park, H.S., Metzger, R., Kowaluk, E., Jarvis, M.F., and van Biesen, T. (1999). *Eur. J. Pharmacol*. **376**, 127-138.

68. Braet, K, Vandamme, W., Martin, P.E.M., Evans, W.H., and Leybaert L. (2003) *Cell Calcium* **33**, 37-48.

FOOTNOTES

We thank Reza Beigi and Dr. Ron Przybylski for discussions and comments and Sylvia Kertesy for technical assistance in tissue culture. This work was supported by NHLBI P01-HL18708 from the National Institutes of Health and Grant-in Aid 9950305N from the American Heart Association (National).

FIGURE LEGENDS

Figure 1. ***Constitutive ATP release and extracellular ATP metabolism by human 1321N1 astrocytes at steady state.*** **A.** Extracellular ATP levels were recorded as described in *Experimental Procedures* at 1-2 min intervals during the initial 100 min following transfer to the luciferase-containing assay medium. At the 100-min time point, a bolus of 100 nM exogenous ATP was added and ATP levels were recorded every 2 min for another 30 min. Digitonin (50 μg/ml) and apyrase (5 U/ml) were added at the end of the assay. Representative single experiment with a 1321N1 monolayer (35 mm dish) assayed at 5 days post plating. **B.** Extracellular ATP was assayed as described in panel A. 1321N1 monolayers were allowed to equilibrate for 45 min prior to treatment with (▲) or without (○) 300 μM βγMeATP. A bolus of 100 nM ATP was then added and ATP levels were recorded every 2 min for another 20 min. Control cell-free dishes (□) containing only BSS were also prepared. Data represents the mean ± SEM from 4 experiments using cell monolayers at 5-7 days post plating. The averaged digitonin-releasable [ATP] was ~4.2 ± 0.4 μM.

Figure 2. ***Effect of ecto-ATPase inhibition on constitutive versus thrombin-induced ATP release.*** **A.** ATP accumulation was recorded in matched 35 mm dishes of confluent 1321N1 monolayers for 10 minutes prior to 20-minute treatments with no added agents (■), 2 U/ml thrombin alone (○) or 300 μM βγMeATP alone (▲). Data represent the mean ± SEM of results from 7 experiments using cell monolayers at 5-7 days post plating. The averaged digitonin-releasable [ATP] was ~6.6 ± 1.3 μM. **B.** ATP accumulation was recorded in matched 35 mm dishes of confluent 1321N1 monolayers

for 10 minutes prior to 20-minute treatments with no added agents (□), 2 U/ml thrombin alone (▲), or thrombin plus 3 (○), 30 (■), 300 (●) μM βγMeATP. Data represent the average ± range from 2 experiments using monolayer at 6-7 days post plating. The averaged digitonin-releasable [ATP] was ~7.3 ± 0.4 μM.

Figure 3. ***PAR1 stimulated release of ATP during ecto-ATPase inhibition: Concentration-response relationships for thrombin versus TRAP agonists.*** **A.** Cell monolayers at 5-6 days post plating were treated with no added agent (●), 300 μM βγMeATP alone (△) or βγMeATP plus 3 (▲), 30 (■), 3000 (□) mU/ml thrombin. **B**. Cell monolayers at 5-6 days post plating were treated with no added agent (○), 300 μM βγMeATP alone (▲) or βγMeATP plus 0. 3 (□), 1 (●), 3 (△) μM TRAP. Data in both A and B represent the mean ± SEM from 3 experiments. The averaged digitonin releasable [ATP] was 4.8 ± 0.1 μM in the panel A experiments and 4.4 ± 0.3 μM in the panel B experiments. **C and D**: The peak extracellular ATP accumulation was plotted as a function of increasing thrombin or TRAP concentration.

Figure 4. ***A strategy for measuring ATP release at the cell surface versus bulk extracellular compartments.*** A scheme showing a method for *in vitro* detection of ATP at the cell surface microenvironment versus the bulk extracellular compartment. The cartoon illustrates how heterologously expressed CD14 is used to tether an immune complex of monoclonal anti-CD14 antibody and proA-luciferase at the 1321N1 cell surface.

Figure 5. ***Kinetics and magnitude of thrombin-induced ATP release at the cell surface of 1321N1 astrocytes.*** 1321N1-CD14 monolayers at 7 days post plating were either coated with anti-CD14 antibody and proA-luc or bathed in soluble luciferase-containing BSS as described in Figs. 1-3. Changes in ATP-dependent luminescence of the adsorbed (▲, △) versus soluble (●, ○) luciferase were measured every ~12 seconds. Following baseline recording, cells were treated for 8 minutes with thrombin in the absence (△,○) or presence (▲, ●) of acutely added 300 μM βγMeATP. Digitonin was then added and ATP measurements were made for a further 3 minutes. (A) and (B) represent independent experiments on single dishes performed on different days but are representative of 4 similar recordings..

Figure 6. ***M1 muscarinic receptor-stimulated accumulation of extracellular ATP in the absence or presence of ecto-ATPase inhibition.*** ATP accumulation was recorded in 35 mm dishes of confluent 1321N1 monolayers for 10 minutes prior to 20-minute treatments with no added agents (■), 100 μM carbachol alone (∀), or 300 μM βγMeATP plus 100 μM carbachol (▼). Data represents the mean $\pm$ SEM of results from 4 experiments using cell monolayers at 5-7 days post plating. The averaged digitonin-releasable [ATP] was 8.7 $\pm$ 0.5 μM.

Figure 7. ***Hypotonic stress-stimulated accumulation of extracellular ATP in the absence or presence of ecto-ATPase inhibition.*** ATP accumulation was recorded in 35 mm dishes of confluent 1321N1 monolayers for 10 minutes prior to 20-minute treatments with no change in extracellular tonicity (■), only a 30% decrease in extracellular tonicity

(○, as described in *Experimental Procedures*), or a 30% decrease in extracellular tonicity plus 300 μM βγMeATP (●). Data represents the mean ± SEM of results from 3 experiments using cell monolayers at 5-7 days post plating. The averaged digitonin-releasable [ATP] was 7.3 ± 0.5 μM.

Figure 8. ***Thrombin and carbachol-stimulated Ca^{2+} transients in control versus BAPTA-loaded 1321N1 astrocytes .*** Parallel aliquots of a 1321N1 cell suspension were preloaded with 1 μM fura2-AM only (Panel A) or with both 1 μM fura2-AM and 10 μM BAPTA-AM (Panel B). Ca^{2+}-dependent changes in fura2 fluorescence were recorded during successive stimulation with 300 μM βγMeATP, 2 U/ml thrombin, or 100 μM carbachol before permeabilization with digitonin. Representative data from a single experiment using cells at 5 days post plating. Similar results were observed in 2 experiments.

Figure 9. ***Effects of BAPTA-loading on constitutive versus stimulated ATP release from 1321N1 astrocytes.*** Extracellular ATP levels in untreated versus BAPTA-AM preloaded monolayers were recorded (as described in previous figure legends) during stimulation by 300 μM βγMeATP alone (panel A), 2U/ml thrombin plus 300 μM βγMeATP (panel B), 100 μM carbachol plus 300 μM βγMeATP (panel C), or a 30% hypotonic stress plus 300 μM βγMeATP (panel D). **A**. Data represent the mean ± SEM of 4 experiments with an averaged digitonin-releasable [ATP] of 6.8 ± 0.8 μM; insert in panel A shows the same data on an amplified Y-axis. **B.** Data represent the mean ± SEM of 7 experiments with an averaged digitonin-releasable [ATP] of 6.7 ± 0.4 μM. **C.** Data

represent the mean ± SEM of 6 experiments with an averaged digitonin-releasable [ATP] of 6.4 ± 0.9 μM. **D.** Data represent the mean ± SEM of 3 experiments with an averaged digitonin-releasable [ATP] of 6.2 ± 0.4 μM.

Figure 10. ***Additive effects of thrombin and hypotonic stress on ATP release from 1321N1 astrocytes.*** ATP accumulation (all in the presence of 300 μM βγMeATP) was recorded in 35 mm dishes of confluent 1321N1 monolayers for 10 minutes prior to 20-minute treatments with 2U/ml thrombin alone (■), a 30% decrease in extracellular tonicity alone (○), or a 30% decrease in extracellular tonicity plus 2U/ml thrombin (●). Data represent the average ± range of 2 experiments with an averaged digitonin-releasable [ATP] of 6.0 ± 0.4 μM.

Table 1.
ATP sensitivity of anti-CD14/protein A-luciferase immune complexes adsorbed to wild type versus CD14-transfected 1321N1 astrocytes

ATP added (nM)	RLU	
	1321N1 wt	1321N1 CD14
0	0.003 +/- 0.003	0.027 +/- 0.016
1	0.013 +/- 0.014	0.019 +/- 0.011
10	0.008 +/- 0.008	0.047 +/- 0.011
100	0.019 +/- 0.014	0.071 +/- 0.019
1000	0.028 +/- 0.017	0.326 +/- 0.064
10000	0.080 +/- 0.005	11.523 +/- 0.639
digitonin	0.101 +/- 0.024	24.637 +/- 7.230

1321N1 wt and 1321N1-CD14 monolayers were serially coated with anti-CD14 monoclonal antibody and proA-luc to determine the CD14 epitope dependence of luciferase binding to the cell surface. Changes in RLU values with increasing concentrations of exogenously added ATP were measured online using single representative dishes. Digitonin (50 μg/ml) was added at the end of the experiment and all recordings were done in triplicate.

Joseph et al Fig 1

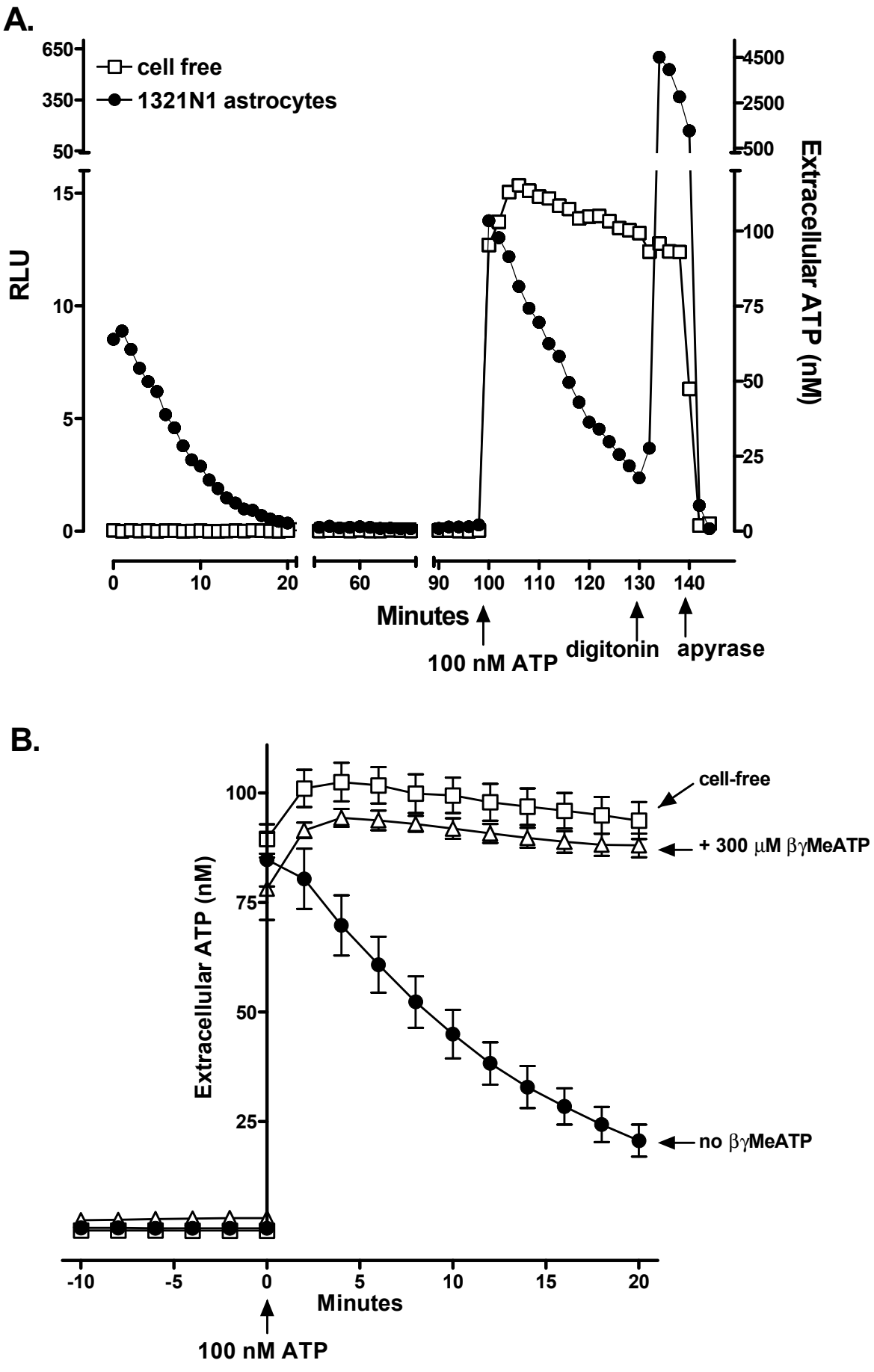

Joseph et al Fig 2

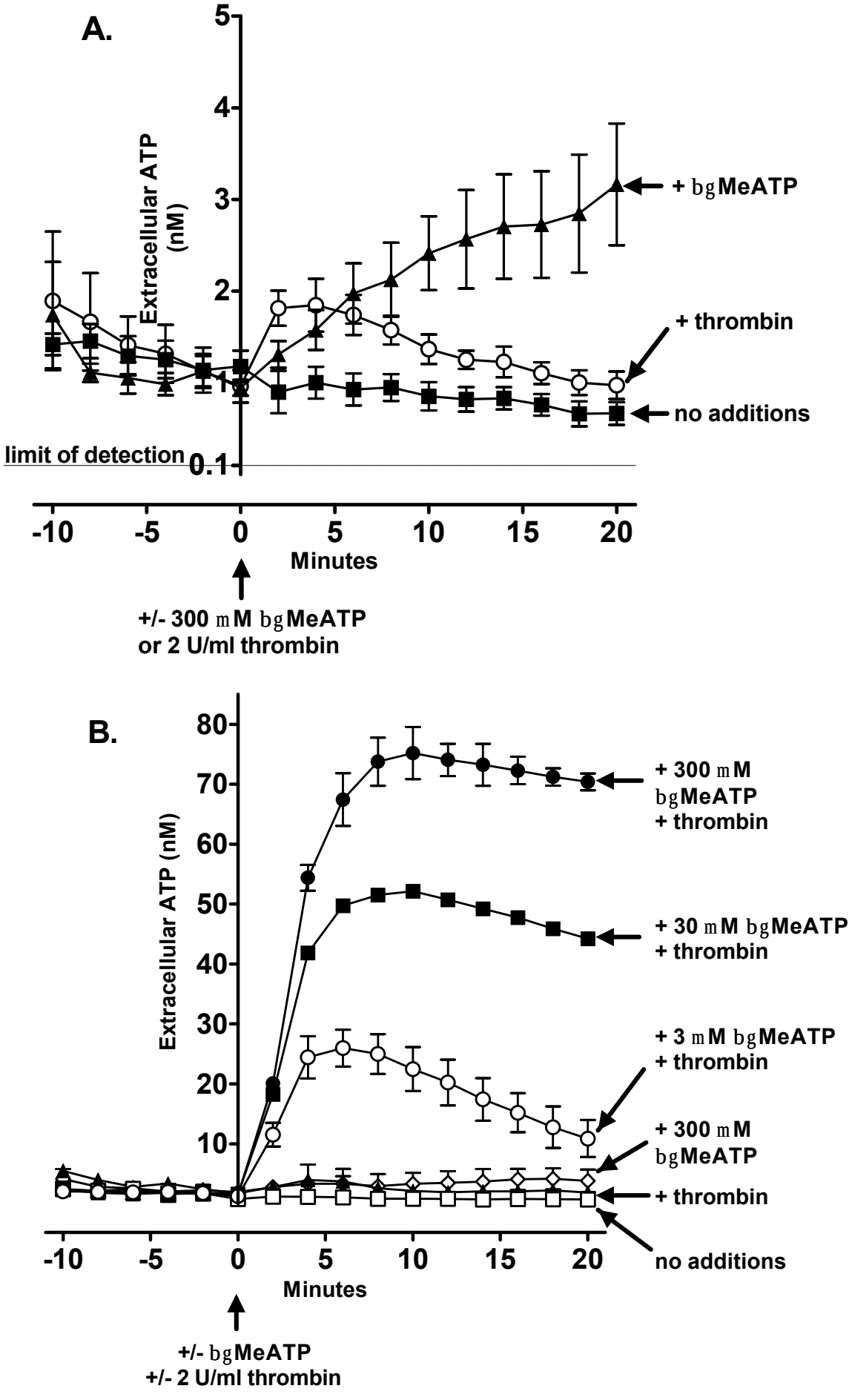

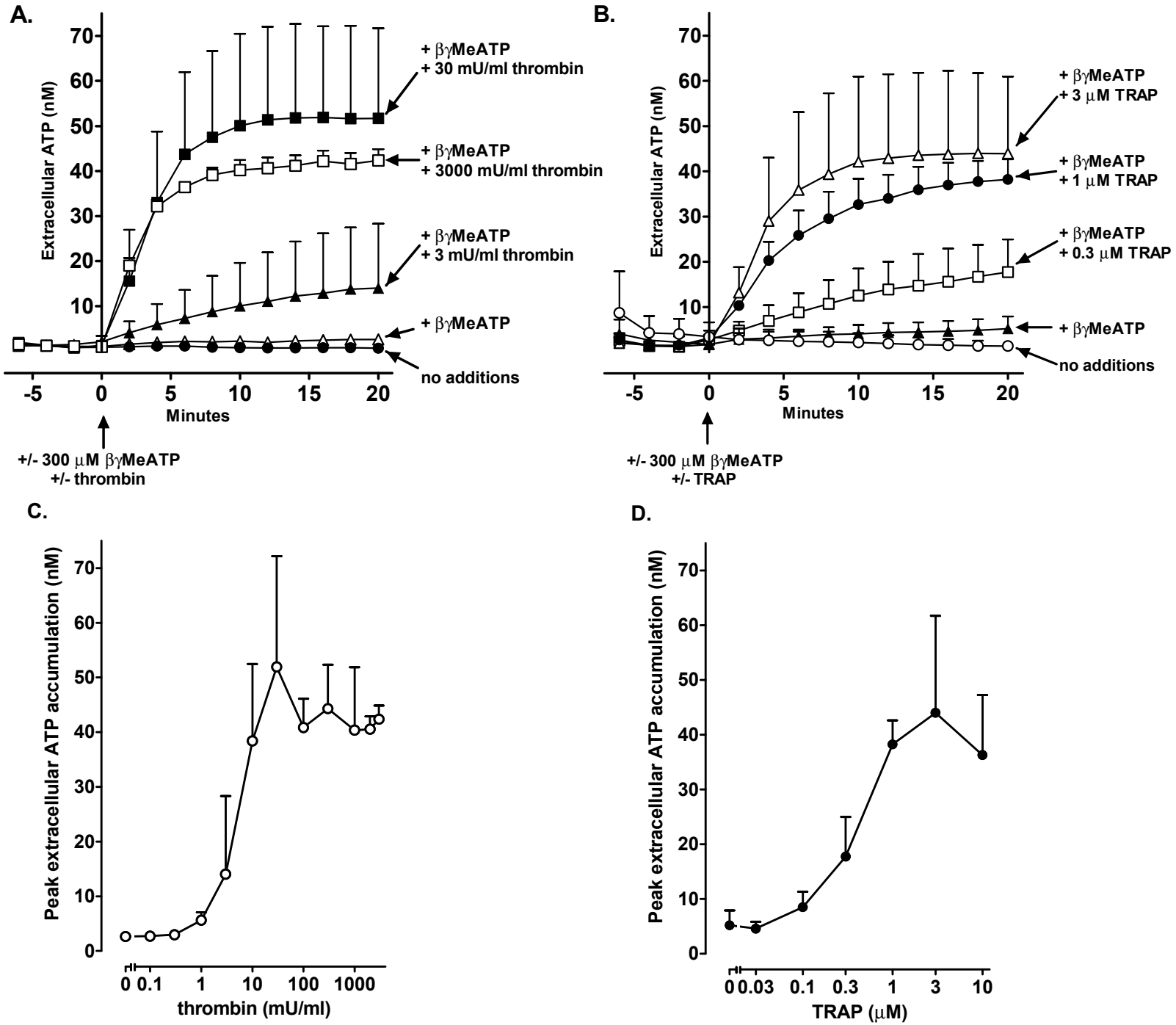
A.
Extracellular ATP (nM)
70
60
50
40
30
20
10
-5
0
5
10
15
20
Minutes
+ βγMeATP
+ 30 mU/ml thrombin
+ βγMeATP
+ 3000 mU/ml thrombin
+ βγMeATP
+ 3 mU/ml thrombin
+ βγMeATP
no additions
+/- 300 μM βγMeATP
+/- thrombin
B.
Extracellular ATP (nM)
+ βγMeATP
+ 3 μM TRAP
+ βγMeATP
+ 1 μM TRAP
+ βγMeATP
+ 0.3 μM TRAP
+ βγMeATP
no additions
Minutes
+/- 300 μM βγMeATP
+/- TRAP
C.
Peak extracellular ATP accumulation (nM)
0
10
20
30
40
50
60
70
0 0.1 1 10 100 1000
thrombin (mU/ml)
D.
Peak extracellular ATP accumulation (nM)
0 0.03 0.1 0.3 1 3 10
TRAP (μM)

Joseph et al Fig 4

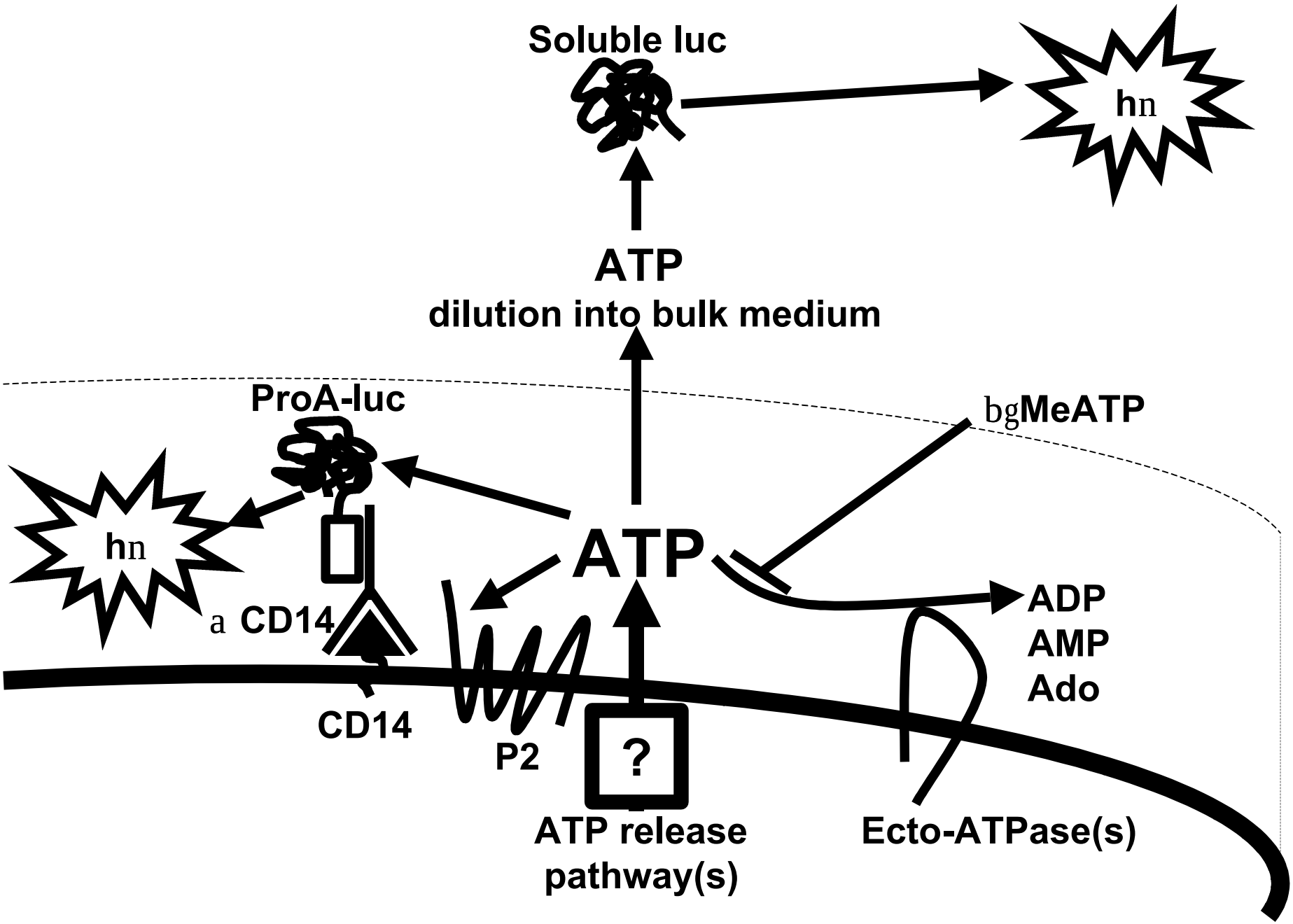

Joseph et al Fig 5

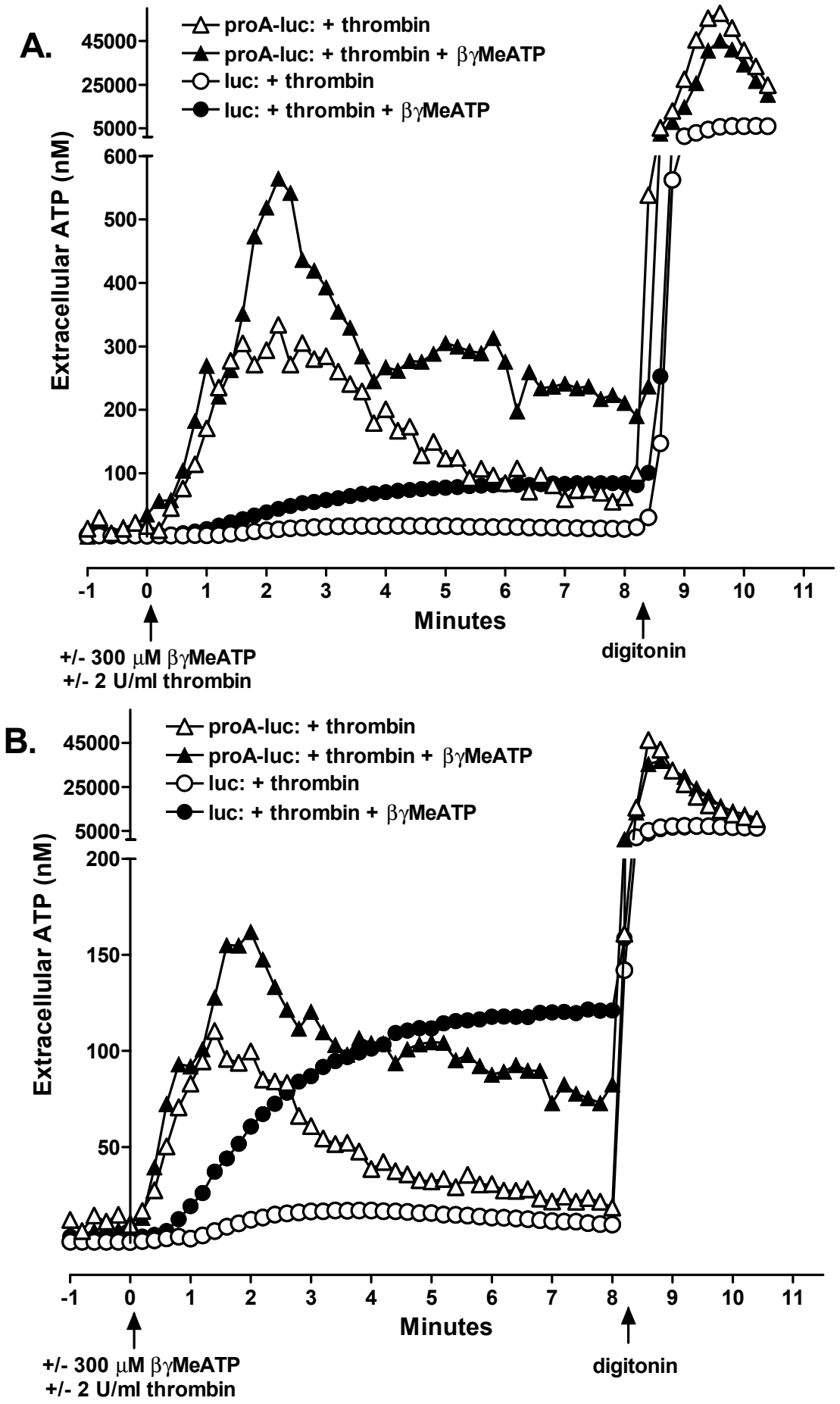

Joseph et al Fig 6

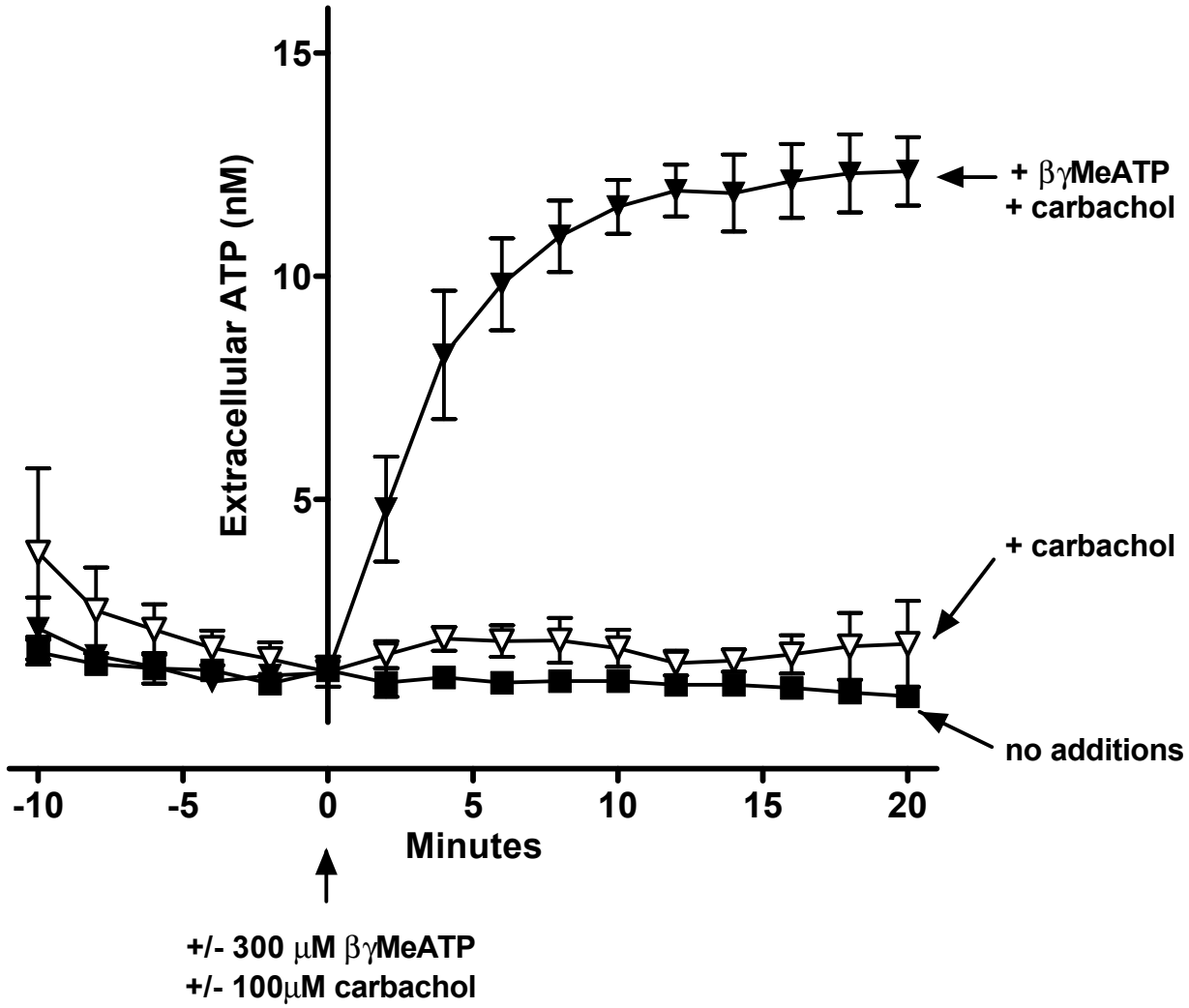

Joseph et al Fig 7

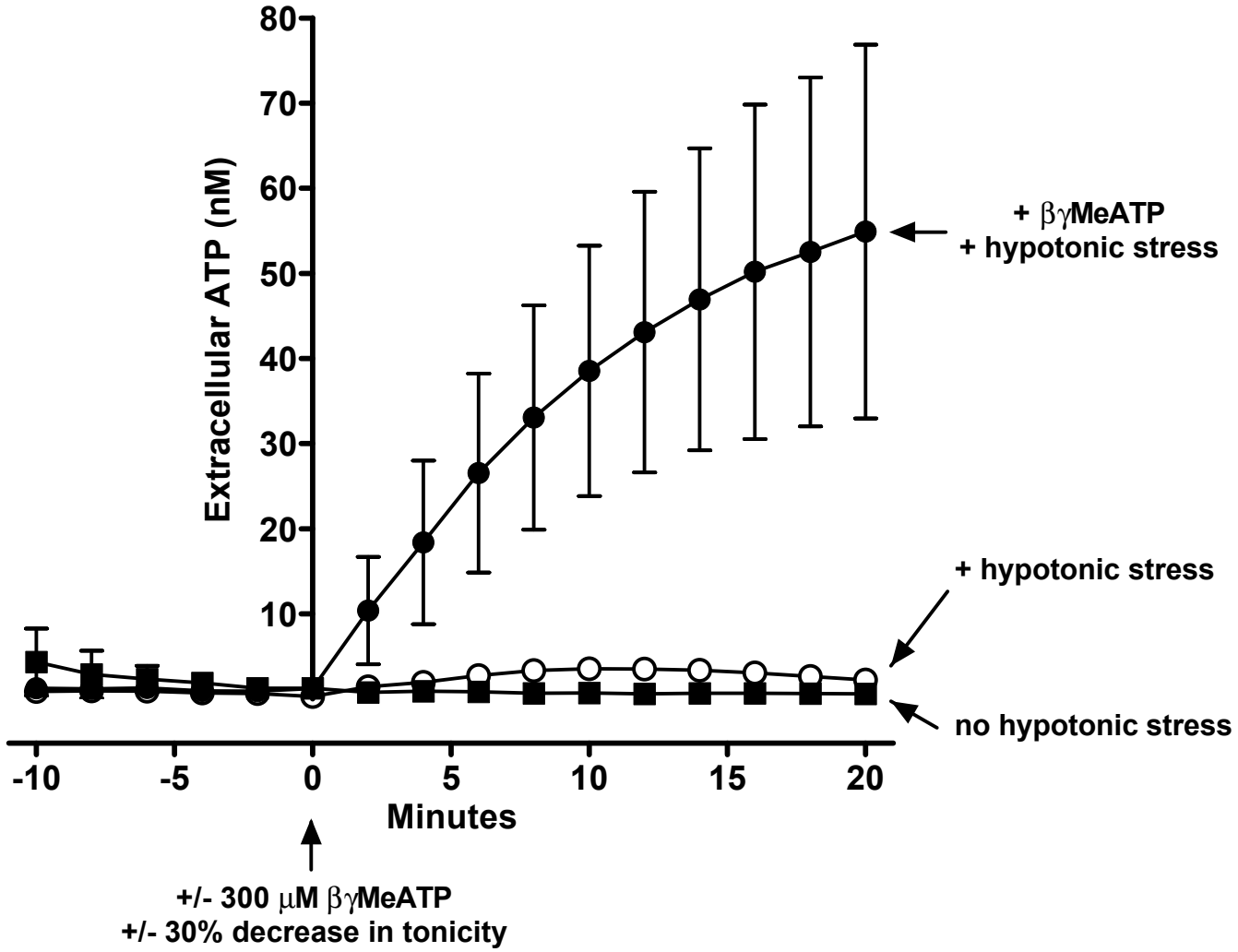

Joseph et al Fig 8

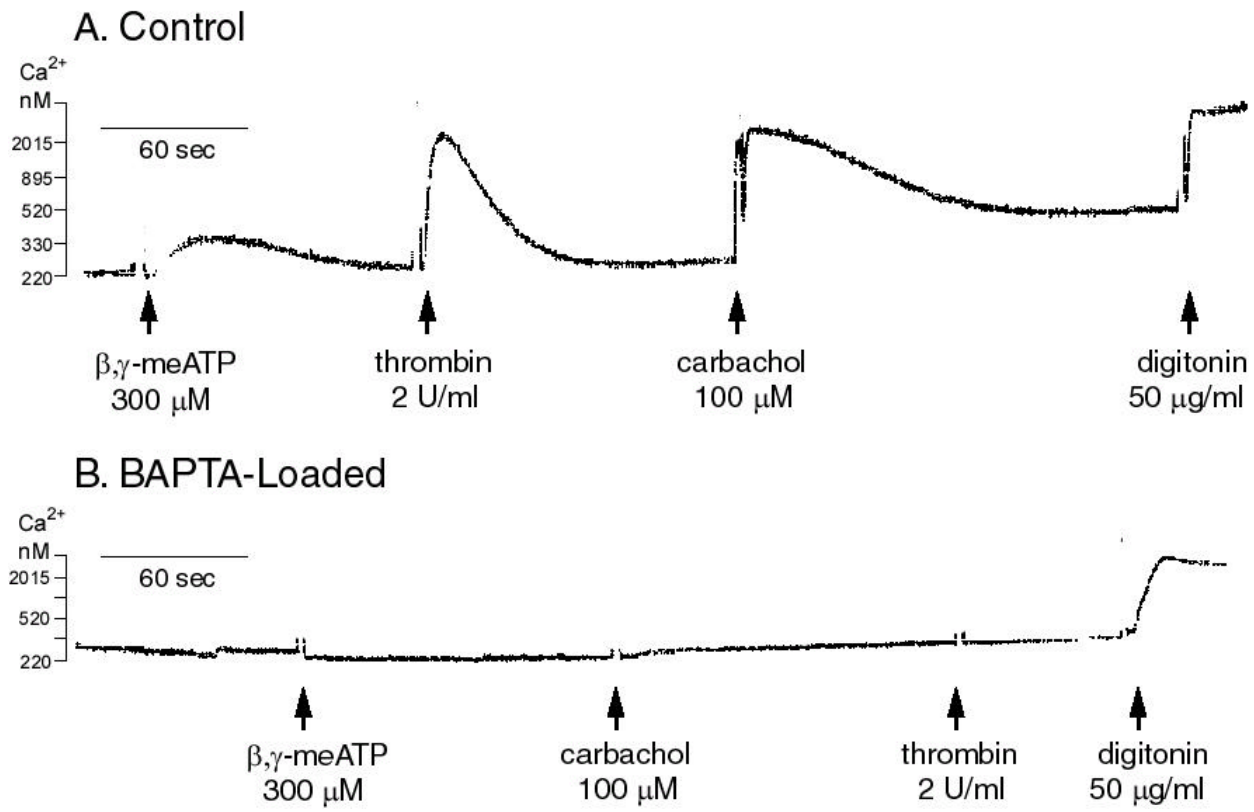

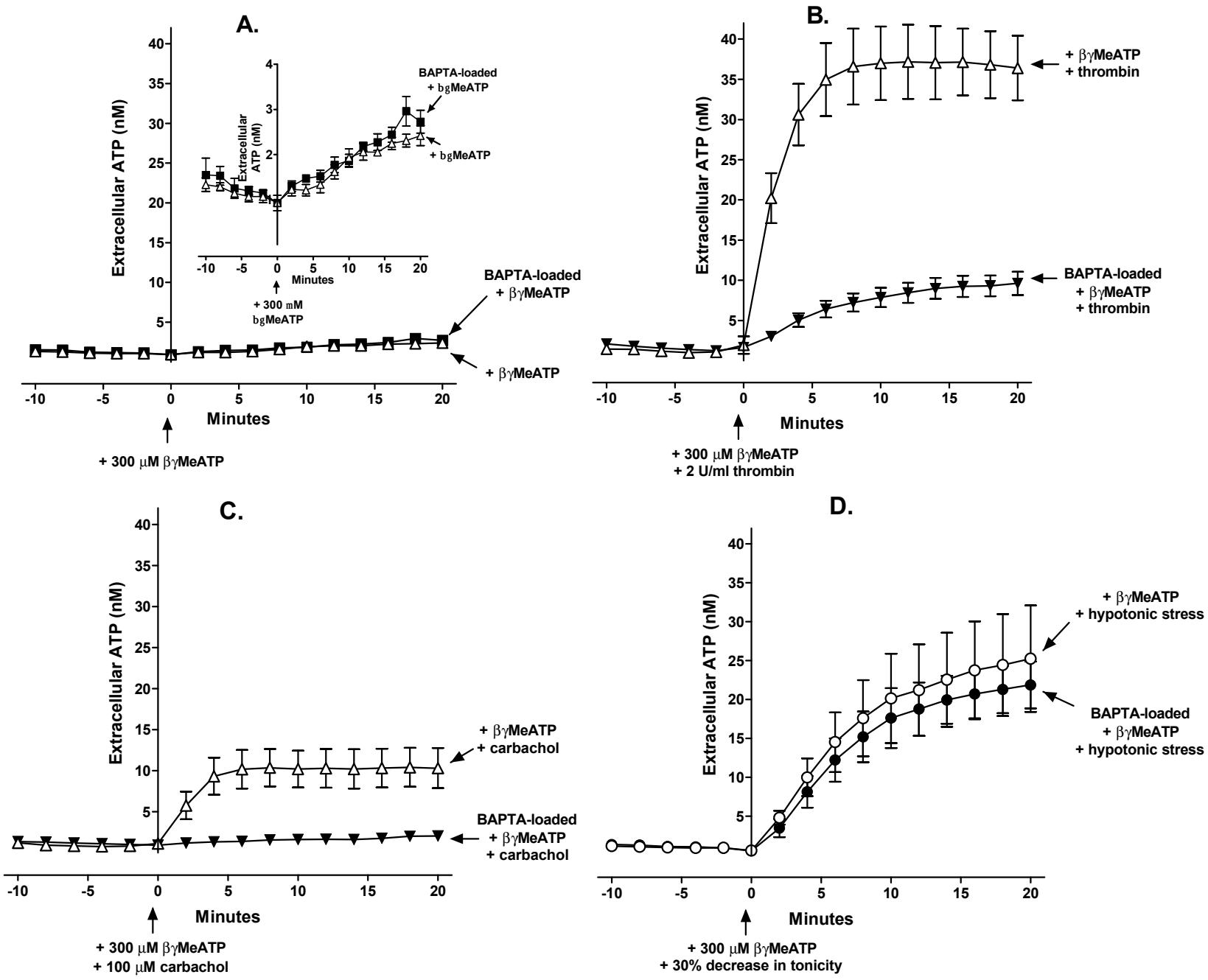
A.
Extracellular ATP (nM)
Minutes
+ 300 μM βγMeATP
BAPTA-loaded
+ βγMeATP
+ βγMeATP
BAPTA-loaded
+ bgMeATP
+ bgMeATP
+ 300 mM
bgMeATP
B.
Extracellular ATP (nM)
Minutes
+ 300 μM βγMeATP
+ 2 U/ml thrombin
+ βγMeATP
+ thrombin
BAPTA-loaded
+ βγMeATP
+ thrombin
C.
Extracellular ATP (nM)
Minutes
+ 300 μM βγMeATP
+ 100 μM carbachol
+ βγMeATP
+ carbachol
BAPTA-loaded
+ βγMeATP
+ carbachol
D.
Extracellular ATP (nM)
Minutes
+ 300 μM βγMeATP
+ 30% decrease in tonicity
+ βγMeATP
+ hypotonic stress
BAPTA-loaded
+ βγMeATP
+ hypotonic stress

Joseph et al Fig 10